

Simple Synthesis of Uniform Mesoporous Carbons with Diverse Structures from Mesostructured Polymer/Silica Nanocomposites

Jinwoo Lee,[†] Jaeyun Kim,[†] Youjin Lee,[†] Songhun Yoon,[‡] Seung M. Oh,[‡] and Taeghwan Hyeon^{*,†}

National Creative Research Initiative Center for Oxide Nanocrystalline Materials, Research Center for Energy Conversion and Storage (RCECS), and School of Chemical Engineering, Seoul National University, Seoul 151-744, Korea

Received July 5, 2003. Revised Manuscript Received May 18, 2004

Uniform-sized mesoporous carbons having high surface areas and various structures were synthesized directly by the carbonization of P123 triblock copolymer/phenol–resin/silica nanocomposites, which were prepared from the sol–gel polymerization of silica in the presence of Pluronic P123 triblock copolymer and phenol and subsequent silica removal. Mesoporous carbon, with uniform 5.6 nm wormhole-like pores, was synthesized using sodium silicate as a silica source. When the amount of phenol relative to block copolymer was reduced in the synthesis, mesocellular carbon foams with bimodal pore structures were obtained. In addition, mesoporous carbons were synthesized using TEOS (tetraethyl orthosilicate) as a silica source. The pore size of the mesoporous carbons was controlled by varying the ratio of phenol and P123 triblock copolymer. At an optimal molar ratio of phenol to block copolymer, mesoporous carbon with a nanofiber morphology was obtained. The mesoporous carbons were successfully used as the electrodes for electrochemical double-layer capacitors.

Introduction

Porous carbon materials have attracted much attention due to their many important applications, for example, as adsorbents, catalyst supports, and electrode materials.^{1,2} Several porous carbon materials have been fabricated using inorganic templates including zeolites,^{3–6} alumina membranes,^{7–9} opal,¹⁰ and silica sols.^{11–14} Porous carbon materials have also been synthesized by copolymerization of a carbon source and silicate

source.^{15,16} More recently, a new class of carbon molecular sieves were synthesized using mesostructured silica (or aluminosilicate) materials as inorganic templates.^{17–32} To date, cubic,^{19–21} disordered,^{22,23} hexagonal,^{24–28} foam-like,^{29,30} and nanopipe^{31,32} type mesostructured carbon materials have been synthesized. Some of these carbon materials have been successfully used as electrodes for electric double-layer capacitors^{19,22} and fuel cells.³¹ Moreover, their good pore connectivity and large pore size (2–30 nm) make these mesoporous carbons attractive catalyst supports. The general synthetic process is as follows: (1) preparation of a mesostructured silica/

* Corresponding author. Fax: +82-2-886-8457. E-mail: thyeon@plaza.snu.ac.kr.

[†] National Creative Research Initiative Center for Oxide Nanocrystalline Materials and School of Chemical Engineering, Seoul National University.

[‡] Research Center for Energy Conversion and Storage (RCECS) and School of Chemical Engineering, Seoul National University.

(1) Rodriguez-Reinoso, F. In *Introduction in Carbon Technology*; Marsh, H., Heintz, E. A., Rodriguez-Reinoso, F., Eds.; Universidad de Alicante, Seerretariado de publicaciones: Alicante, 1997; p 35.

(2) *Proceedings of The Symposium on Electrochemical Capacitors*; Delnick, F. M., Tomkiewicz, M., Eds.; The Electrochemical Society: Pennington, 1996.

(3) Johnson, S. A.; Brigham, E. S.; Olliver, P. J.; Mallouk, T. E. *Chem. Mater.* **1997**, *9*, 2448.

(4) Kyotani, T.; Nagai, T.; Inoue, S.; Tomita, A. *Chem. Mater.* **1997**, *9*, 609.

(5) Ma, Z.; Kyotani, T.; Tomita, A. *Chem. Commun.* **2000**, 2365.

(6) Ma, Z.; Kyotani, T.; Liu, Z.; Terasaki, O.; Tomita, A. *Chem. Mater.* **2001**, *13*, 4413.

(7) Kyotani, T.; Tsai, L.; Tomita, A. *Chem. Mater.* **1995**, *7*, 1427.

(8) Kyotani, T.; Tsai, L.; Tomita, A. *Chem. Mater.* **1996**, *8*, 2109.

(9) Che, G.; Lakshimi, B. B.; Fisher, E. R.; Martin, C. R. *Nature* **1998**, *393*, 347.

(10) Zakhidov, A. A.; Baughman, R. H.; Iqbal, Z.; Cui, C.; Khayrullin, I.; Dantas, S. O.; Marti, J.; Ralchenko, V. G. *Science* **1998**, *282*, 897.

(11) Han, S.; Hyeon, T. *Carbon* **1999**, *37*, 1645.

(12) Han, S.; Sohn, K.; Hyeon, T. *Chem. Mater.* **2000**, *12*, 3337.

(13) Han, S.; Hyeon, T. *Chem. Commun.* **1999**, 1955.

(14) Li, Z.; Jaroniec, M. *J. Am. Chem. Soc.* **2001**, *123*, 9208.

(15) Han, S.; Lee, K. T.; Oh, S. M.; Hyeon, T. *Carbon* **2003**, 1049.

(16) Kawashima, D.; Aihara, T.; Kobayashi, Y.; Tomita, A. *Chem. Mater.* **2000**, *12*, 3397.

(17) Lee, J.; Han, S.; Hyeon, T. *J. Mater. Chem.* **2004**, *14*, 478.

(18) Ryoo, R.; Joo, S. H.; Kruk, M.; Jaroniec, M. *Adv. Mater.* **2001**, *13*, 677.

(19) Lee, J.; Yoon, S.; Hyeon, T.; Oh, S. M.; Kim, K. B. *Chem. Commun.* **1999**, 2177.

(20) Ryoo, R.; Joo, S. H.; Jun, S. *J. Phys. Chem. B* **1999**, *103*, 7743.

(21) Yoon, S. B.; Kim, J. Y.; Yu, J.-S. *Chem. Commun.* **2001**, 559.

(22) Lee, J.; Yoon, S.; Oh, S. M.; Shin, C.-H.; Hyeon, T. *Adv. Mater.* **2000**, *12*, 359.

(23) Lee, J.; Kim, J.; Hyeon, T. *Chem. Commun.* **2003**, 1138.

(24) Jun, S.; Joo, S. H.; Ryoo, R.; Kruk, M.; Jaroniec, M.; Liu, Z.; Ohsuna, T.; Terasaki, O. *J. Am. Chem. Soc.* **2000**, *122*, 10712.

(25) Kim, S.-S.; Pinnavaia, T. J. *Chem. Commun.* **2001**, 2418.

(26) Yu, C.; Fan, J.; Tian, B.; Zhao, D.; Stucky, G. D. *Adv. Mater.* **2002**, *14*, 1742.

(27) Lu, A.; Kiefer, A.; Schmidt, W.; Schüth, F. *Chem. Mater.* **2004**, *16*, 100.

(28) Li, Z.; Jaroniec, M. *J. Phys. Chem. B* **2004**, *108*, 824.

(29) Lee, J.; Sohn, K.; Hyeon, T. *J. Am. Chem. Soc.* **2001**, *123*, 5646.

(30) Lee, J.; Sohn, K.; Hyeon, T. *Chem. Commun.* **2002**, 2674.

(31) Joo, S. H.; Choi, S. J.; Oh, I.; Kwak, J.; Liu, Z.; Terasaki, O.; Ryoo, R. *Nature* **2001**, *412*, 169.

(32) Zhang, W.-H.; Liang, C.; Sun, H.; Shen, Z.; Guan, Y.; Ying, P.; Li, C. *Adv. Mater.* **2002**, *14*, 1776.

surfactant nanocomposite, which often takes 2–3 days; (2) the removal of the surfactant by calcination or solvent extraction; (3) the generation of catalytic sites inside the wall of the mesostructured silica for subsequent polymerization (in some synthesis); (4) incorporation of polymer precursor, such as phenol, furfuryl alcohol, or sucrose into the pores of the mesoporous silica material; (5) polymerization to obtain a carbon precursor; (6) carbonization; and finally, (7) the removal of the silica template using HF or NaOH solution. This long and complicated multistep template synthetic procedure hampers the broad application of these mesostructured carbons, despite their many important characteristics, and a short and simple synthetic procedure is required if such materials are to achieve widespread use. Recently, Moriguchi and co-workers reported the direct synthesis of mesoporous carbon materials by the in situ polymerization of divinylbenzene in the hydrophobic phase of a hexagonally arrayed micelle/silica nanocomposite and its subsequent carbonization and HF treatment.³³ However, the carbon structure achieved only ~2 nm wormhole-like mesopores, which will limit the extensive applications. Yu and co-workers reported the direct preparation of mesoporous carbons using as-synthesized MCM-48 silica/surfactant nanocomposite,³⁴ but an additional carbon precursor, poly(divinylbenzene), was synthesized inside the empty space of the silica/surfactant composite after the preparation of a mesostructured MCM-48 silica/surfactant nanocomposite. Sayari and co-workers reported the direct preparation of wormhole-like mesoporous carbon through the carbonization of a silica/cyclodextrin-template nanocomposite.³⁵ The carbon material produced was a disordered wormhole-like microporous material. In our continuous effort to develop a new simple synthetic procedure for mesoporous carbons with connected and uniform pores, we used a combination of the triblock copolymer Pluronic P123 and the carbon precursor phenol as a structure-directing agent. Herein, we report on the synthesis of mesoporous carbons with uniformly sized three-dimensionally interconnected mesopores having various hierarchical structures from the carbonization of nanocomposites composed of silica, P123 triblock copolymer, and phenol resin, followed by silica removal.

Experimental Section

Direct Synthesis of Mesoporous Carbon Materials Using Sodium Silicate as a Silica Source. In a typical synthesis, 4 g of P123 ((EO)₂₀(PO)₇₀(EO)₂₀) and an appropriate amount of phenol was dissolved in 150 mL of 1.6 M HCl solution and heated to 40 °C for 6 h. Then 6.8 mL of sodium silicate solution (6.8 mL; 27% SiO₂, 14% NaOH, Aldrich Chemical Co.) diluted with 10 mL of H₂O was poured into the solution with vigorous stirring, and then 3 equiv of formaldehyde solution (73% w/w) relative to the amount of phenol present was added to the solution and heated at 60 °C for 2 h. The opaque solution obtained was then transferred to a screw-capped polypropylene bottle and was aged at 100 °C for 2 h under a static condition and allowed to cool to room temperature. The red precipitate formed, a phenol resin-P123/silica

composite, was isolated by filtration, dried in air, and carbonized by heating at 800 °C for 3 h in a nitrogen atmosphere. The silica component was then dissolved by stirring in a 5 wt % HF at room temperature to generate mesoporous carbon, designated Direct-C-S (the S indicates that the silica source was sodium silicate). The difference of synthetic method for the Direct-C-S and Direct-C-S-1 is the amount of phenol that is added in the synthetic gel. When the amount of phenol was reduced to three-fourths of that used for the synthesis of Direct-C-S, Direct-C-S-1 was obtained.

Direct Synthesis of Mesoporous Carbon Materials Using TEOS as a Silica Source. The difference from the synthetic procedure using sodium silicate as a silica source is longer polymerization time. After 3 equiv of formaldehyde solution (37% w/w) relative to the amount of phenol was added to H₂O solution containing P123 and HCl, the temperature of the solution was increased to 60 °C and kept at this temperature for 12 h. The opaque light-red solution obtained was then transferred to a screw-capped polypropylene bottle and aged at 100 °C for 24 h under static conditions. The remaining process is the same as that described for Direct-C-S. The resulting carbon was designated Direct-C-T (T represents TEOS). The difference in the synthetic method for the Direct-C-T-1 and Direct-C-T-2 is the amount of phenol that is added in the synthetic gel. When the amount of phenol was reduced to three-fourths of that used for the synthesis of Direct-C-T, Direct-C-T-1 was obtained. When the amount of phenol was further reduced to half of that used for the synthesis of Direct-C-T, Direct-C-T-2 was obtained.

Characterization of Materials. Materials were characterized by nitrogen sorption, transmission electron microscopy (TEM), and scanning electron microscopy (SEM). TEM images were obtained using a Philips CM-20 unit and SEM images using a JSM-840A. N₂ adsorption/desorption isotherms at 77 K were obtained using a Micromeritics ASAP2010 sorptometer. Pore size distributions were calculated using the BJH (Barett–Joyner–Harenda) method. To prepare the EDLC electrodes, a mixture of carbon, poly(tetrafluoroethylene) (PTFE) binder, and Ketjenblack ECP-600JD (10:2:1 wt:wt) was dispersed in isopropyl alcohol and coated on 1 cm × 1 cm stainless steel Exmet, which was used as the current collector. The resulting electrode plate was pressed and dried under vacuum at 120 °C for 12 h. The EDLC performance of the composite carbon electrodes was analyzed using a three-electrode configuration in aqueous 2.0 M H₂SO₄ electrolyte. A Pt flag and SCE (saturated calomel electrode) were used as counter and reference electrodes, respectively. Cyclic voltammetric and chronoamperometric measurements were taken using an EG&G PARC 362 potentiostat in the potential range of 0.0–0.7 V (vs SCE).

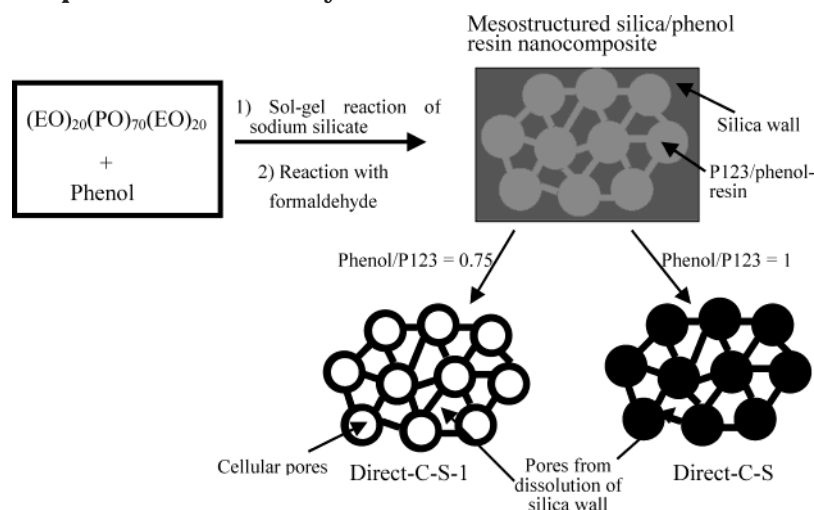
Results and Discussion

The overall synthetic procedure is described in Scheme 1. Sol–gel polymerization of silica in the presence of Pluronic P123 triblock copolymer and phenol generated a P123/phenol/silica nanocomposite. A combination of triblock copolymer and phenol was used as the structure-directing agent. The addition of formaldehyde to the P123/phenol/silica nanocomposite generated a P123/phenol–resin/silica nanocomposite. HCl was used as the catalyst for both the sol–gel reaction of silica and for the synthesis of the phenol resin. Carbonization followed by the removal of the silica component using HF produced the final mesoporous carbon materials. The removal of silica was examined by energy-dispersive X-ray analysis (EDX) measurement, and the elemental analysis data are supplied in Table 1. In all carbon materials, the remaining Si is less than 0.5% of atomic ratio, which shows the silica materials were successfully removed from the carbon/silica composite. Carbons with uniform mesopores are derived from silica walls with

(33) Moriguchi, I.; Koga, Y.; Matsukura, R.; Teraoka, Y.; Kodama, M. *Chem. Commun.* **2002**, 1844.

(34) Yoon, S. B.; Kim, J. Y.; Yu, J. S. *Chem. Commun.* **2002**, 1536.

(35) Han, B.-H.; Zhou, W.; Sayari, A. *J. Am. Chem. Soc.* **2003**, *125*, 3444.

Scheme 1. Schematic Representation of the Synthetic Procedure for Direct-C-S and Direct-C-S-1 Carbons**Table 1. Elemental Analysis Data of Direct Templated Carbons by Energy Dispersive X-ray Spectroscopy**

sample	carbon (%)	oxygen (%)	silicon (%)
Direct-C-S	95.54	4.04	0.42
Direct-C-S-1	96.05	3.48	0.47
Direct-C-T	95.90	3.94	0.16
Direct-C-T-1	94.94	4.64	0.42
Direct-C-T-2	95.40	3.92	0.12

uniform thickness. The structural properties of the resulting mesoporous carbons are summarized in Table 2.

Synthesis of Mesoporous Carbons Using Sodium Silicate as a Silica Source. The structure of mesoporous Direct-C-S carbon, which was synthesized from the carbonization of the P123/phenol–resin/silica nanocomposite prepared under strongly acidic conditions using sodium silicate as a silica source, was investigated by gas adsorption measurements and TEM. The nitrogen adsorption/desorption isotherms of Direct C-S showed two hysteresis curves at relative pressure of $\sim 0.7 P/P_0$ and $\sim 0.95 P/P_0$, respectively. The pore size distribution (PSD) of Direct-C-S calculated using the BJH (Barrett–Joyner–Halenda) method showed pores centered at 5.6 nm (Figure 1a). The surface area and pore volume of Direct C-S were 1080 m²/g and 1.0 cm³/g, respectively. The steep increase at $\sim 0.95 P/P_0$ was the result of textural interparticle pores generated between primary particles. Because the phenol resin/P123/silica composite was assembled using a prehydrolyzed sodium silicate as a silica source, small-sized mesostructured particles are synthesized along with large-sized mesostructured particles. When sodium silicate was used as a silica

source, prehydrolyzed sodium silicate was added to highly acidic solution. On addition of the sodium silicate to the acidic solution containing block copolymer, the condensation of silicic acid occurs immediately. Because the hydrolyzed sodium silicate passes the neutral condition before achieving highly acidic conditions, the fast growth will occur in a near neutral pH. The mesostructured particle seeds are formed both in the neutral pH and in the final acidic medium. The seeds formed at the neutral condition seemed to lead to the formation of small-sized particles because the condensation rate of silicic acid is very high under a near neutral pH (around ~ 6.5).^{36,37} These small individual particles seemed to generate interparticle pores. In contrast, large-sized particles seemed to be produced from the seeds formed under the final acidic conditions because the condensation rate of silanol in acidic conditions is slow. The coexistence of the small and large particles is clearly shown in the SEM image (Figure 1c).

The uniformity of the mesopores in Direct C-S seems to result from the uniformity of the thickness of the silica framework in the carbon/silica composite because pores are generated by the dissolution of the silica framework in the silica/carbon nanocomposite. The uniformity of silica wall thickness demonstrates the intimate interaction among the silica, the block copolymer, and phenol. In the current synthetic strategy to obtain uniform-sized mesoporous carbons, P123 with phenol was used as the structure-directing agent for assembling the silica. The majority of mesoporous silica materials synthesized using surfactant self-assemblies as templates possess a uniform wall thickness, which

Table 2. Pore Characteristics of Direct-C's Prepared Using Various Phenol/P123 Weight Ratios and Using Different Silica Sources

	phenol:P123 weight ratio	silica source	pore structure	surface area (m ² /g)	BJH pore diameter (nm)	mesoporosity ^e
Direct-C-S	1:1	S ^a	unimodal	1077	5.57	0.40
Direct-C-S-1	3:4	S	bimodal	1308	12.5/2.74 ^c	1.01
			mesocellular foam		8.92/2.52 ^d	
Direct-C-T	3:2	T ^b	unimodal	702	3.87	0.61
Direct-C-T-1	1:1	T	unimodal	678	4.48	1.02
Direct-C-T-2	3:4	T	unimodal nanofiber	1080	3.14	0.96

^a Sodium silicate (14% NaOH, 27% SiO₂). ^b Tetraethyl orthosilicate (TEOS). ^c From adsorption branches. ^d From desorption branches. ^e Mesoporosity is defined as the ratio $S_{\text{BJH}}/S_{\text{BET}}$.

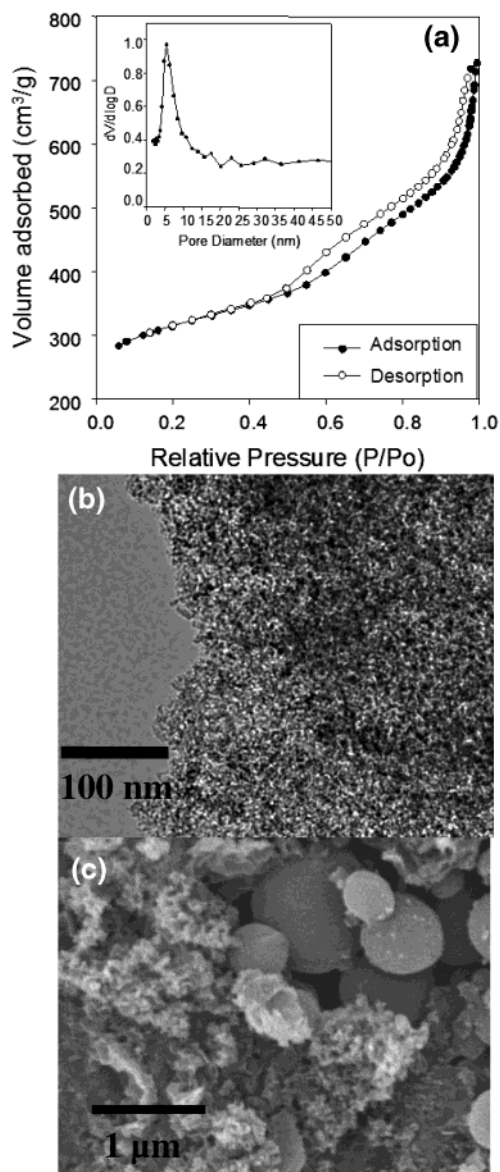


Figure 1. (a) Nitrogen adsorption/desorption isotherms of Direct-C-S. Inset: Corresponding pore size distribution calculated from N_2 adsorption data using BJH (Barrett–Joyner–Halender) method. (b) TEM image of Direct-C-S. (c) SEM image of Direct-C-S.

is also derived from the intimate interaction between surfactant and silica. Phenol seems to be present dominantly at the interface between propylene oxide and ethylene oxide regions in the P123 triblock copolymer, presumably because of its hydrophilic character.³⁸ Consequently, after carbonization, some carbon fraction, which was mixed with part of a PEO fraction, seems to penetrate the complementary pores of the mesostructured silica.³⁹ This carbon fraction in the complementary pores retains the mesostructure framework of the final mesoporous carbon materials even after the removal of the silica framework (Scheme 1). The N_2 adsorption/

desorption isotherms of Direct-C-S/silica nanocomposite showed no steep increase at $0.7 P/P_0$, demonstrating that the pores are completely filled with carbon materials (see Supporting Information). The TEM image of Direct-C-S carbon, shown in Figure 1b, showed ~ 5 nm sized pores. The pore structure was disordered and wormhole-like, which is similar to that of HMS and HMS-templated carbon.²² But the pore size of Direct-C-S is larger than that of HMS-templated carbon by about 3.5 nm. The wall thickness of MCF⁴⁰ and SBA-15⁴¹ silica materials synthesized using high molecular weight triblock copolymers as templates is larger than that of mesoporous silica materials synthesized using low molecular weight surfactants such as cetyltrimethylammonium bromide (CTAB).^{42,43} As a result, the pore sizes of mesoporous carbon materials synthesized using SBA-15 and MCF silica templates are usually larger than those of mesoporous carbon materials made using HMS and MCM-48 silica templates. In the present study, triblock copolymer P123 and phenol were used as the structure-directing agent, which makes a thicker silica wall.

Recently, new mesocellular carbon foams with pore sizes ranging from 20 to 30 nm have been synthesized by our group using mesocellular silica foam and MSU-F silica materials as templates.^{29,30} Prior to our group's report on mesocellular carbon foams, the pore sizes of mesoporous carbons synthesized using mesostructured silica templates were limited to 2–4 nm because these pores were generated from the dissolution of the silica wall of the templates. In the current work, we synthesized mesocellular carbon foams (Direct-C-S-1) with a bimodal pore structure by simply reducing the relative amount of phenol to block copolymer. The nitrogen adsorption/desorption isotherms of Direct-C-S-1 show two hystereses at $\sim 0.3 P/P_0$ and $\sim 0.85 P/P_0$ (Figure 2a). The increase at $\sim 0.3 P/P_0$ is attributed to the small mesopores inside the walls of the mesocellular carbon foam and the hysteresis loop at $0.7–0.9 P/P_0$ to the large cellular mesopores. The pore size distribution of the mesocellular carbon foam, calculated from the adsorption branch of the isotherms using the BJH (Barrett–Joyner–Halender) method, exhibited two different pores centered at 12.5 and 2.7 nm, which resulted from the main cells and the mesopores present in the carbon wall, respectively (Figure 2b). Pore size analysis derived from the desorption branch of the isotherms showed a bimodal pore arrangement with pores centered at 8.9 and 2.5 nm, which were generated from the windows of the main cells and the mesopores present in the carbon wall, respectively (Figure 2c). The BET surface area and single-point total pore volume of Direct-C-S-1 are $1310 \text{ m}^2/\text{g}$ and $1.5 \text{ cm}^3/\text{g}$, respectively. Mesoporous carbons, prepared using mesoporous silicas as templates, generally possess micropores inside the carbon walls.^{20,22} The micropore volume of Direct-C-S-1 as determined by the Horvath–Kawazoe method was $0.50 \text{ cm}^3/\text{g}$. These micropores were generated by the carbonization of phenol

(36) Kim, S.-S.; Karkamkar, A.; Pinnavaia, T. J.; Kruk, M.; Jaroniec, M. *J. Phys. Chem. B* **2001**, *105*, 7663.

(37) Kim, S.-S.; Pauly, T. R.; Pinnavaia, T. J. *Chem. Commun.* **2000**, 1661.

(38) Lettow, J.-S.; Han, Y.-J.; Schmidt-Winkel, P.; Yang, P.; Zhao, D.; Stucky, G. D.; Ying, Y. J. *Langmuir* **2000**, *16*, 8291.

(39) Kruk, M.; Jaroniec, M.; Ko, C. H.; Ryoo, R. *Chem. Mater.* **2000**, *12*, 1961.

(40) Schmidt-Winkel, P.; Lukens, W.-W., Jr.; Yang, P.; Margolese, D. I.; Lettow, J. S.; Ying, J. Y.; Stucky, G. D. *Chem. Mater.* **2000**, *12*, 686.

(41) Zhao, D.; Feng, J.; Huo, Q.; Melosh, N.; Fredrickson, G. H.; Chmelka, B. F.; Stucky, G. D. *Science* **1998**, *279*, 548.

(42) Tanev, P. T.; Pinnavaia, T. J. *Science* **1995**, *267*, 865.

(43) Kreszege, C. T.; Leonowicz, M. E.; Roth, W. J.; Vartuli, J. C.; Beck, J. S. *Nature* **1992**, *359*, 710.

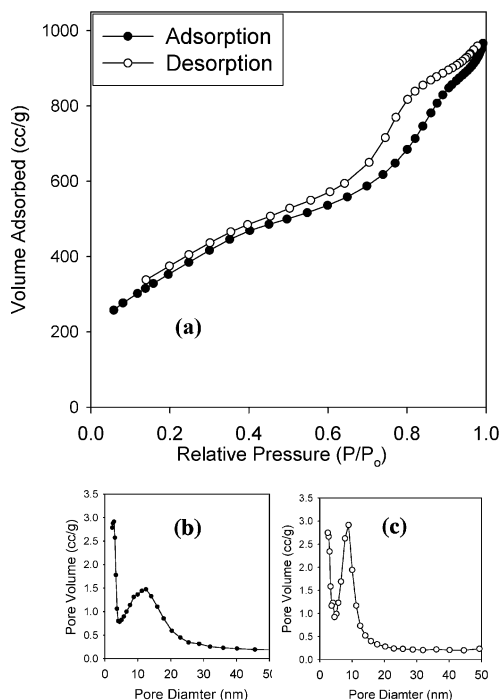


Figure 2. (a) Nitrogen adsorption/desorption isotherms of Direct-C-S-1. (b) Corresponding pore size distribution calculated from N_2 adsorption data using BJH (Barrett–Joyner–Halender) method. (c) Corresponding pore size distribution calculated from N_2 desorption data using BJH (Barrett–Joyner–Halender) method.

resin.²² Mesoporosity, defined as S_{BJH}/S_{BET} , was increased from 0.40 (Direct-C-S) to 1.01 (Direct-C-S-1) by reducing the ratio of phenol to silica. The N_2 isotherms of the Direct-C-S-1/silica nanocomposite before HF etching were similar to those of Direct-C-S-1, except for the absence of a small hysteresis at 0.3 P/P_0 (see Supporting Information). The absence of hysteresis at $\sim 0.3 P/P_0$ indicates that the small mesopores are generated by the dissolution of the silica wall. The pore size distribution of Direct-C-S-1/silica composite shows unimodal pores centered at around 11 nm, which indicate that the large cellular pores are generated by the carbonization of phenol–resin/silica composite and that the small ~ 2.5 nm pores are generated by the dissolution of silica walls. Reducing phenol seems to generate voids in the PPO/phenol resin (Scheme 1). The TEM image of Direct C-S-1 at low magnification showed about 15 nm sized holes (Figure 3), but the pore uniformity of these large cellular pores was not as evident as those of MCF carbon²⁹ or MSU-F-C.³⁰ At higher magnification, two distinct pore structures were observed, that is, ~ 15 nm cellular pores and ~ 2.5 nm wormhole-like pores, respectively. The current synthetic procedure for mesocellular carbon foam is simpler than those based on the use of MCF and MSU-F as silica templates and hopefully will trigger extensive applications of the mesocellular carbon materials as catalyst supports, adsorbents, and electrode materials.

Synthesis of Mesoporous Carbons Using TEOS as a Silica Source. Mesoporous Direct-C-T carbons were synthesized from the carbonization of the P123/phenol–resin/silica nanocomposite prepared under strongly acidic conditions using TEOS as a silica source. Direct-C-T has uniformly sized mesopores centered at

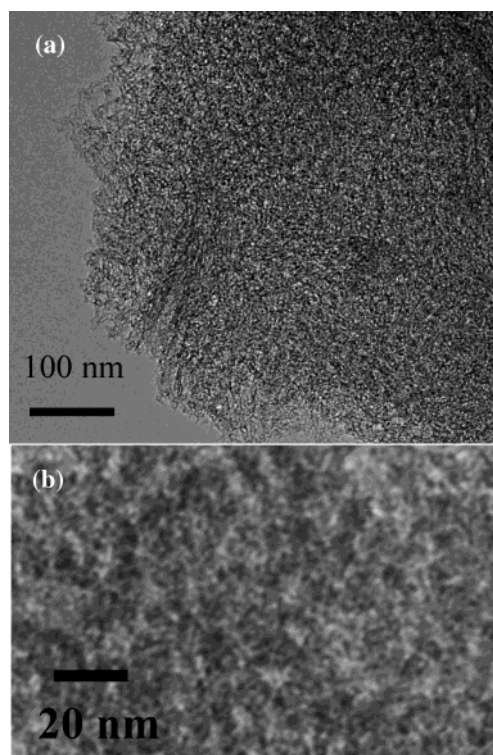


Figure 3. TEM image of Direct-C-S-1 (a) at low magnifications and (b) at high magnifications.

3.9 nm. The significantly smaller amount of adsorption at a P/P_0 of ~ 0.95 in the N_2 isotherm compared to that of Direct-C-S carbon indicates that Direct-C-T is composed of monolithic large particles (Figure 4a). This large particle size was confirmed by the SEM image of Direct-C-T (Figure 4c). The BET surface area and the single-point total pore volume of Direct-C-T are $700 \text{ m}^2/\text{g}$ and $0.67 \text{ cm}^3/\text{g}$. TEM studies of Direct-C-T show uniform 4 nm pores (Figure 4b). The pore structure is also wormhole-like and similar to that of Direct-C-S.

Recently, the nanofiber-structured porous materials were synthesized by several groups.^{44–47} Until now, nanotubes of silica,⁴⁴ rare earth oxides,⁴⁵ and alumina^{45,46} have been synthesized. For the formation of nanofiber- or nanotube-structured porous materials, the surfactant packing factor of the synthetic system is known to be between 1/3 and 1/2, which is responsible for the hexagonal packing.⁴⁴ The synthetic condition for Direct-C-T-2 seems to match the condition. Because the condensation rate is much slower than the hydrolysis rate in highly acidic conditions, an extensive packing of the individual surfactant/silica nanofiber seems to be prevented, consequently generating separated nanofibers.⁴⁴ In the present study, by controlling the relative amount of phenol to block copolymer, mesoporous carbon with a nanofiber morphology, designated as Direct-C-T-2, was obtained. The N_2 adsorption/desorption isotherms of Direct-C-T-2 exhibited a well-developed steep capillary condensation step at a pressure of

(44) Harada, M.; Adachi, M. *Adv. Mater.* **2000**, *12*, 839.

(45) Yada, M.; Mihara, M.; Mouri, S.; Kuroki, M.; Kijima, T. *Adv. Mater.* **2002**, *14*, 309.

(46) González-Peña, V.; Díaz, I.; Márquez-Alvarez, C.; Sastre, E.; Pérez-Pariente, J. *Microporous Mesoporous Mater.* **2001**, *44–45*, 203.

(47) Lee, H. C.; Kim, H. J.; Chung, S. H.; Lee, K. H.; Lee, H. C.; Lee, J. S. *J. Am. Chem. Soc.* **2003**, *125*, 2882.

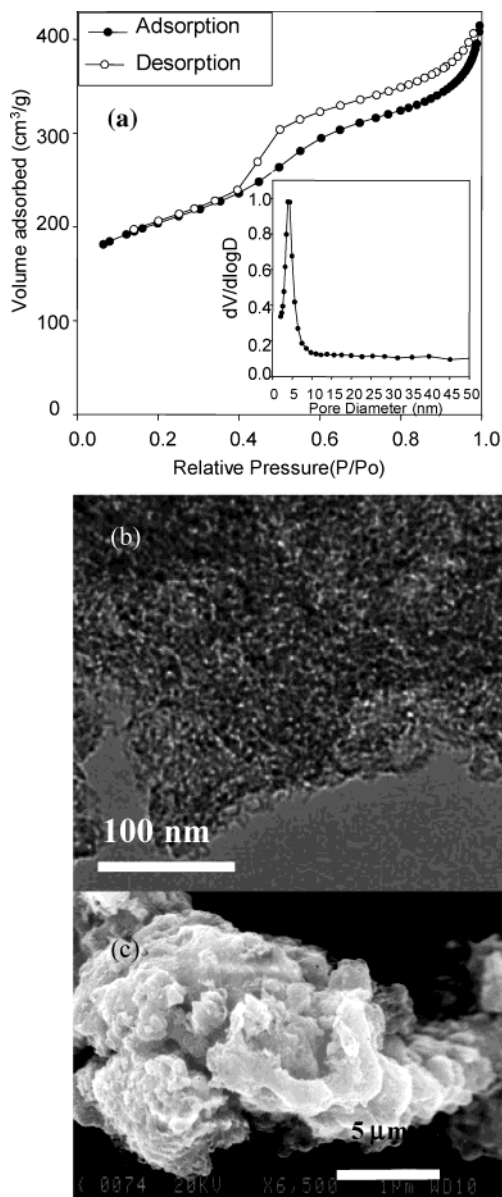


Figure 4. (a) Nitrogen adsorption/desorption isotherms for Direct-C-T. Inset: Corresponding pore size distribution calculated from BJH (Barrett–Joyner–Halender) theory on the basis of N_2 adsorption data. (b) TEM image of Direct-C-T. (c) SEM image of Direct-C-T.

$\sim 0.5 P/P_0$, indicating a narrow mesopore size distribution (Figure 5a). The pore size of Direct-C-T-2 was 3.14 nm. The BET surface area and single-point total pore volume of Direct-C-T-2 were $1080 \text{ m}^2/\text{g}$ and $0.95 \text{ cm}^3/\text{g}$, respectively. Mesoporosity, defined as $S_{\text{BJH}}/S_{\text{BET}}$, was also increased from 0.61 (Direct-C-T) to 0.96 (Direct-C-T-2) by reducing the relative amount of phenol to silica. TEM image revealed that Direct-C-T-2 is a nanofiber-type porous material (Figure 5b,c). The diameter of some mesoporous nanofibers was about 50 nm. These 50 nm sized nanofibers possess uniform mesopores, the direction of which is parallel to the direction of the nanofibers. This is the first synthesis of uniform mesoporous carbon with a nanofiber morphology, and its synthesis is simpler than the syntheses of other nanotubular or nanofiber mesoporous materials. Pore size control of mesoporous carbons using TEOS as the silica source for the silica/phenol resin nanocom-

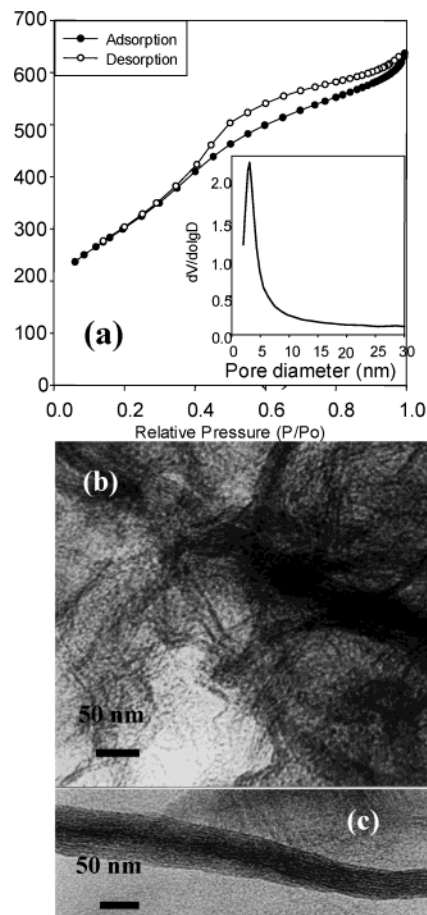


Figure 5. (a) Nitrogen adsorption/desorption isotherms for Direct-C-T-2. Inset: Corresponding pore size distribution calculated from BJH (Barrett–Joyner–Halender) theory on the basis of N_2 adsorption data. (b) TEM image of Direct-C-T-2 at low magnifications and (c) at high magnifications.

posite was achieved easily by varying the relative amount of phenol to silica. In contrast, pore size control of template-synthesized carbons is usually difficult because the pore size of the mesoporous carbon is determined by the wall thickness of the mesoporous silica templates. Recently, Ryoo and co-workers produced template-synthesized mesoporous carbons with pore sizes controllable in a narrow region from 2.2 to 3.3 nm by controlling the wall thickness of the template mesoporous silica.⁴⁸ The pore size of Direct-C-T-1 using phenol and P123 at a weight ratio of 1:1 was 4.5 nm. As described above, the pore sizes of Direct-C-T and Direct-C-S were 3.1 and 5.5 nm, respectively. Consequently, we were able to control the pore sizes of these directly synthesized mesoporous carbons from 3.1 to 5.5 nm.

Applications of Mesoporous Carbons to the Electrode Materials for Electrochemical Double-Layer Capacitors (EDLC). Mesoporous carbons have been applied to the electrodes for electrochemical double-layer capacitors (EDLCs). EDLCs utilize the electric double layer formed at the electrode/electrolyte interface for charge storage. In order for porous carbons to have a high charge storage capability, they should first have a large surface area since charge storage ability (ex-

(48) Lee, J.-S.; Joo, S. H.; Ryoo, R. *J. Am. Chem. Soc.* **2002**, *124*, 1256.

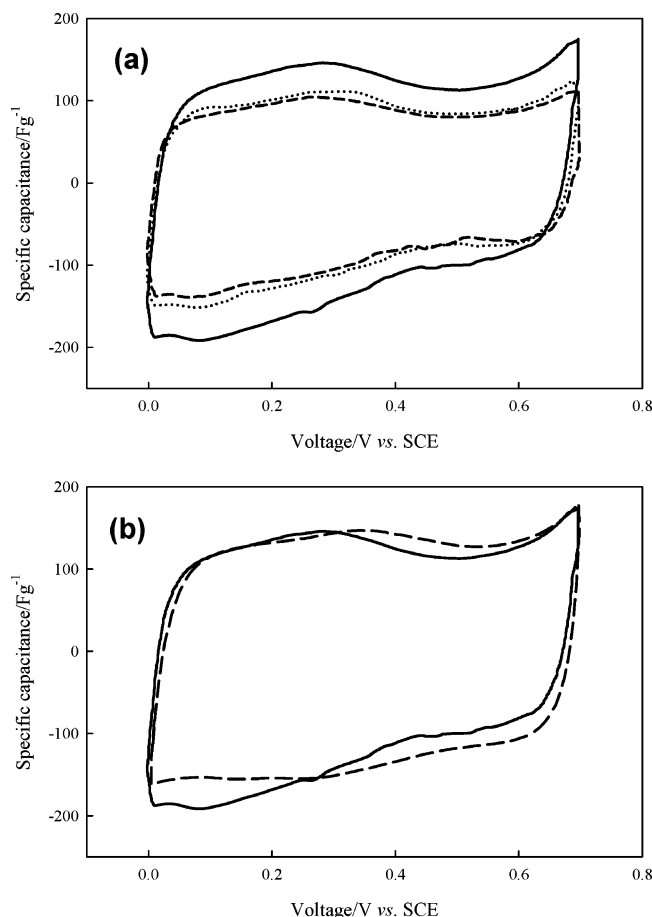


Figure 6. Potential-dependent capacitance profiles. These profiles were obtained after dividing the currents in cyclic voltammograms by the scan rate. Scan rate = 5 mV s^{-1} . (a) The solid line, dotted line, and dashed line are Direct-C-S-1, Direct-C-T, and Direct-C-T-1, respectively. (b) The solid line and dashed line are Direct-C-S-1 and SNU-2, respectively.

pressed as capacitance) is proportional to surface area. The rate capability is another important consideration for practical EDLC because a complete charging of the electric double layer is not always guaranteed. Incomplete utilization of electrode surfaces occurs particularly in high current (rate) conditions when ionic motions in the electrolyte are slower than current transient. This undesirable feature is more pronounced when pores are narrow, long, and irregularly connected as ions cannot penetrate into the deeper regions, and therefore, surface exposed there may not be utilized for charge storage. The ideal EDLC electrode materials can thus be envisaged as those that have a large surface area and large pores, a short length, and good pore connectivity—even if some of these properties conflict. Recently, ordered mesoporous carbons obtained through mesostructured silica templates were used as electrode materials for electrochemical double-layer capacitors (EDLC). Electrodes of MCM-48 and HMS-templated carbons showed a higher rate capability than MCS-25 activated carbon electrodes due to a smaller RC time constant, which is evidenced by both the more rectangular-shaped cyclic voltammograms and capacitance vs voltage profiles.^{19,22,49} The smaller RC time constant was mainly due to a lower

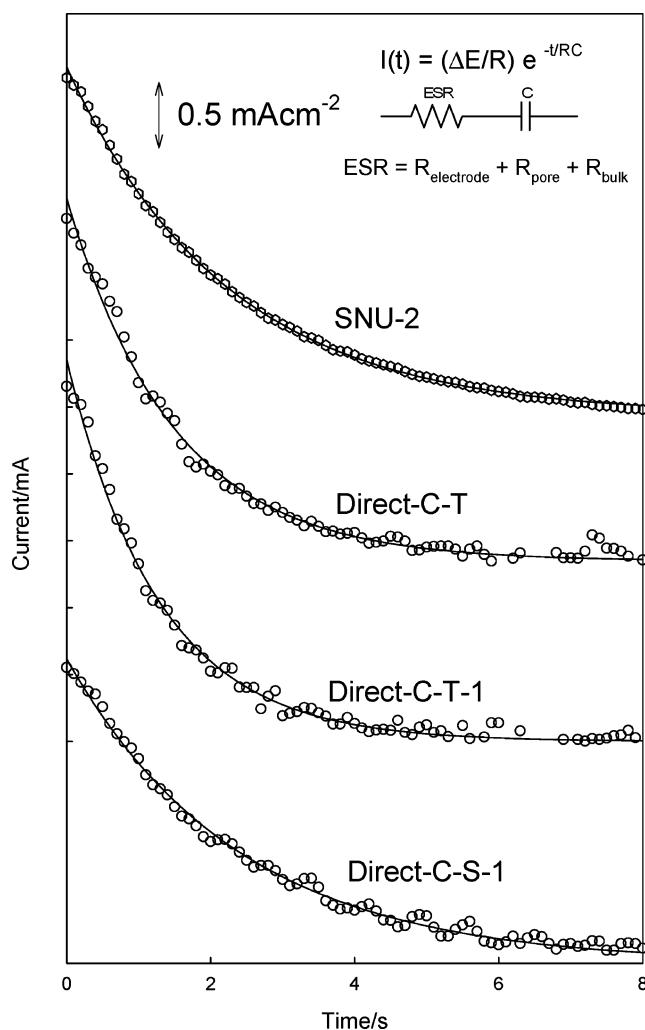


Figure 7. Typical current transient from a chronoamperometry experiment. A potential step (10 mV) was applied from 0.2 V(vs SCE). Individual current data were shifted for easy comparison. The equivalent circuit is depicted in the inset. The empty circles are the observed current transient and the solid lines represent the best fit with equation indicated in the inset.

electrolyte resistance in its pores, resulting from the large size of mesopores and their regular interconnection. Although the applications of ordered mesoporous carbons produced from mesostructured silica template were successful, as already mentioned, the production cost is expected to be very high because the synthetic scheme is complex. Direct templated carbons as prepared here were therefore used as EDLC electrode materials.

Figure 6 shows the capacitance vs voltage profiles of Direct-C-S-1 and Direct-C-Ts. Capacitance was calculated by dividing the measured current by the scan rate (5 mV/s). All direct-templated carbons and HMS-templated mesoporous carbon (SNU-2) exhibited typical capacitor behavior by having rectangular-shaped (mirror image) $I-V$ curves. The specific capacitances of the individual carbon materials are clearly shown in this figure. Pseudocapacitance also appeared at 0.3–0.4 V (vs SCE), which is related to charge-transfer reactions at the surface quinone/hydroquinone groups.⁴⁹ To estimate the equivalent series resistance (ESR), the RC time constants of Direct-C-S-1, Direct-C-Ts, and SNU-2 were determined by chronoamperometry. For this mea-

(49) Yoon, S.; Lee, J.; Oh, S. M.; Hyeon, T. *J. Electrochem. Soc.* **2000**, *147*, 2507.

Table 3. Specific Capacitance, Pore Resistance (R_{pore}), and Time Constant Obtained from a Chronoamperometry Experiment

	capacitance ^a (F g ⁻¹)	R_{pore}^b (Ω cm ²)	time constant ^c (s)
SNU-2	132	2.84	2.27
Direct-C-S-1	135	2.52	2.38
Direct-C-T	101	2.90	1.49
Direct-C-T-1	96	2.76	1.28

^a Measure value from cyclic voltammetry at 0.2 V vs SCE under scan rate of 5 mV/s (Figure 6). ^b R_{pore} was calculated from extraction of $R_{\text{electrode}}$ and R_{bulk} from ESR in Figure 7. ^c Data from fitting of value of chronoamperometry by equation depicted in Figure 7.

surement, a potential step (10 mV) was applied from 0.2 V, and the resulting current transients were recorded. This base potential (0.2 V) was selected because the pseudocapacitance arising from the quinone–hydroquinone redox reaction is absent in this potential range (Figure 6). In Figure 7, current transients obtained from chronoamperometry experiments on Direct-C-S-1, Direct-C-Ts, and SNU-2 are presented. The exponentially decaying current transients were fitted to the equation $I(t) = (\Delta E/R)e^{-t/\tau}$, from which the ESR (R) and capacitance (C) values were obtained. In Figure 7, the equivalent circuit is depicted in the inset. Here, ESR is comprised of $R_{\text{electrode}}$, R_{pore} , and R_{bulk} .⁴⁹ The capacitance and the ESRs estimated from fitting are presented in Table 3. The capacitances of Direct-C-S-1 are comparable to those of SNU-2 in the range from 110 to 130 Fg⁻¹. The higher capacitances certainly stem from the higher surface areas of Direct-C-S-1, compared with Direct-C-T and Direct-C-T-1. The ESRs of the direct templated carbons were as low as that of SNU-2. Because $R_{\text{electrode}}$ and R_{bulk} are fixed for all electrodes, ESR differences mainly stem from R_{pore} and are indicative of the better pore structure of direct-templated

carbons for facile ionic transport. The fact that the ESRs of direct-templated carbons are comparable to SNU-2, which have 3-D interconnected pores, indirectly reveals that they possibly have 3-D interconnected pore structures.

Conclusion

Wormhole-like mesoporous carbons, mesocellular carbon foams with bimodal pore structures, and nanofiber-type mesoporous carbons were synthesized directly from the carbonization of P123 triblock copolymer/phenol–resin/silica nanocomposites, followed by the removal of the silica. These mesoporous carbon materials exhibited high surface areas and uniform pore size distributions. The current synthetic procedure is much simpler than the general template synthetic method, which uses mesoporous silicas as nanoscopic templates. Many time-consuming steps including surfactant extraction, alumination, and the incorporation of polymeric precursors are skipped. The EDLC performance of some of the Direct-Cs is comparable to SNU-2,²² HMS-templated carbon. It is hoped that this simple synthetic method will encourage the extensive applications of mesoporous carbons to other electrode materials, to catalyst supports, and as adsorbents for large molecules.

Acknowledgment. We would like to thank the National Creative Research Initiative Program of the Korean Ministry of Science and Technology for the financial support. We thank Prof. Chae-Ho Shin at the Chungbuk National University for the micropore structure characterization.

Supporting Information Available: Additional figures (PDF). This material is available free of charge via the Internet at <http://pubs.acs.org>.

CM034588V